Journal of the European Ceramic Society 22 (2002) 2261–2268

www.elsevier.com/locate/jeurceramsoc

# Ultrasonic measurements as an in situ tool for characterising the ageing of an aluminous cement at different temperatures

A. Smith[a,*], T. Chotard[a,b,*], N. Gimet-Breart[a], D. Fargeot[a,b]

[a]*Groupe d'Etude des Matériaux Héterogènes (GEMH, EA 3178) Ecole Nationale Supérieure de Céramique Industrielle, 47 à 73 Avenue Albert Thomas, 87065 Limoges Cedex, France*

[b]*Institut Universitaire de Technologie Département Genie Mécnique et Productique, 2 allée André Maurois, 87065 Limoges Cedex, France*

Received 8 June 2001; received in revised form 29 November 2001; accepted 28 December 2001

**Abstract**

In situ ultrasonic measurements have been done to characterise the ageing of a calcium aluminate cement, namely Secar 71, between 24 to 3500 h (5 months) after mixing the constituents. The longitudinal velocity, $V_L$, has been measured on pastes prepared at 5, 20, 40 and 60 °C with a water over cement weight ratio, $W/C$, equal to 0.33. These in situ and real time data are compared with ex situ measurements such as DTA, XRD and porosimetric characterisations. DTA and XRD permit to follow the chemical and crystallographic changes occurring in the material during hydration. The variations of $V_L$ as a function of porous volume fraction, $P$, show that the relation between these two parameters is linear if $P<0.15$ and $V_L>4300$ m/s. When $P>0.15$ and $V_L<4300$ m/s, the relationship between $V_L$ and $P$ is no longer linear; the variations of $V_L$ as a function of $P$ depend on many other parameters such as chemical nature of interfaces, nature of hydrates, morphology of crystals. 

*Keywords:* Ageing; Calcium aluminate cement; Cements; Hydration mechanisms; Ultrasonic characterisation

## 1. Introduction

When mentioning calcium aluminate cements, one thinks about mechanical strength of refractory concretes.[1] However, strength is not the only significant parameter.[2] It is essential that every concrete structure should continue to perform its intended functions, that is maintain its required strength and serviceability, during the specified or traditionally expected service life. Such concrete is said to be durable.

In previous papers,[3,4] we have presented the characterisation of early hydration by in situ measurements of the ultrasonic longitudinal wave velocity and of the associated reflection coefficient. We have shown that this technique is adapted to follow the stiffening of the paste and also the crystallisation of hydrates. The ultrasonic velocity data have been fitted with a dissolution and precipitation model to explain the formation of hydrates in an aluminous cement paste.[5] The present study is focussed on the mechanical behaviour of the cement from 24 h up to 5 months (3500 h) after mixing the constituents. Though a complete study of durability is not the purpose of the present paper, we wish to discuss the effect of temperature (namely 5, 20, 40 and 60 °C) on the long term behaviour of an aluminous cement (from 24 to 3500 h).

The tested material contains no chemical admixture and no constituents such as sand or gravels; we wish to focus specifically on the hydration behaviour of the cement paste alone. The physical and chemical characterisations are based on ultrasonic measurements and also on XRD, DTA and mercury porosimetry. The role of chemical interfaces between the different phases on the propagation of the ultrasonic waves is also discussed.

## 2. Experimental

### 2.1. Preparation of the cement paste and characterisation

The cement is a commercial aluminous material (Secar 71). The results presented here refer to one cement manufactured at a given date and stored for a

* Corresponding author.
*E-mail addresses:* a.smith@ensci.fr (A. Smith), t.chotard@ensci.fr (T. Chotard).

0955-2219/02/$ - see front matter 
PII: S0955-2219(02)00003-1

short period. The study of the early hydration (up to 24 h) of the same cement is discussed in a previous paper.[5] Different lots are prepared with this raw material. Mixing is carried out at different temperatures, namely 5, 20, 40 and 60 °C, according to the normalised procedure N° CEN 196–3. Prior to mixing, the constituents are kept at the mixing temperature. Each lot of paste is prepared with a water-to-cement weight ratio ($W/C$) equal to 0.33. After mixing, the paste is poured in a polymethylmethacrylate (PMMA) mould where it is for 24 h. Then, the set samples are stored in water at the same temperature as the initial one. These samples are noted 05.033, 20.033, 40.033 and 60.033.

Between 0 and 24 h, the samples are characterised with an experimental set-up already described elsewhere.[3,4] The dimensions of the PMMA mould ($100\times50\times10$ mm) are specifically suited to operate in a semi-infinite mode condition (central frequency of the transducer: 1 MHz, average particle size of the cement powder: 10 μm, $\lambda$ (wavelength) $<<$ dimensions of the mould and $\lambda$ (wavelength) $>>$ average particle size). The transit time, $t$ (in s), through the cement sample is related to its thickness, $e$, and the velocity of longitudinal wave, $V_L$ (m/s), as follows:

$$V_L = \frac{2e}{t} \quad (1)$$

The experimental error on $V_L$ is of the order of 2%. From 24 to 3500 h, ultrasonic characterisations are done by immersion. In this case, the sample is immersed into water which acts as a wave guide. The measured parameter is $V_L$. It should be noted that this method does not allow a sufficiently precise estimation of the reflection coefficient $R$, since the error is of the order of 15–20%. Ex situ characterisations of the material have also been done by thermal analysis and XRD at increasing times. Prior to these characterisations, cement hydration is stopped by a mixture of ethanol and ether in a 1:1 volume ratio.[6] Water that is not trapped in hydrates is removed. The resulting product is ground prior to thermal (DTA and TGA) or X-ray diffraction (XRD) analyses. XRD has been conducted with an INEL CPS 120-curved position sensitive diffractometer. Thermal analysis has been carried out with a DTA-TG coupled Rigaku thermoflex; each experiment has been done on 96 mg of product under dry nitrogen with a heating ramp of 15 °C/mm. The reference material is a calcined alumina from Prolabo. The quantity of bound water, which is trapped in the hydration products, was estimated from weight losses recorded by TG measurements at 1000 °C. Lastly, mercury porosimetry has been performed on set samples (model Autopore II Micrometrics 9200). Though this method has some limitations since it cannot provide a true pore size distribution,[7–9] or it indicates smaller than actual porosity where pores are too small or too isolated to be intruded by mercury, it may be closer to actual values than those indicated by other techniques such as helium picnometry. In the present case, mercury porosimetry gives information about the pore volume fraction, $P$, and the pore size distribution.

## 3. Results and discussion

The velocity data between 0 and 24 h are given here for comparison with values recorded between 24 and 3500 h (Fig. 1). A complete discussion of the $V_L$ variations as a function of time between 0 and 24 h has been developed in.[5] The main conclusions are the following:

(i) at any temperature, the velocity remains low (close to the longitudinal velocity in water) and fairly constant at the beginning where the quantity of formed hydrates is low. The ultrasonic waves travel across a water like medium. This first step is the nucleation phase. The higher the temperature is, the shorter is the duration of the nucleation phase: it goes from about 10, 4, 1 h 30 min to 30 min when the experiment is carried out at 5, 20, 40 and 60 °C;
(ii) in a second step, the velocity increases notably and reaches fairly similar values at 24 h, of the order of 3800 m/s, whatever the temperature is. At this point, the chemical nature of formed hydrates, which depends on the temperature, has a little influence upon the values of $V_L$.

It is now interesting to examine the variations of $V_L$ after 24 h and once the samples are immersed in water. Three typical behaviours can be distinguished depending on $T_{exp}$:

(i) at 5 °C, $V_L$ increases with a low rate. It reaches 4500 m/s at 2000 h and a slight decrease can be noted between 2000 and 3500 h.
(ii) at 20 °C, $V_L$ increases with a slightly more important rate. $V_L$ is equal to 5000 m/s at 3500 h.
(iii) at 40 and 60 °C, $V_L$ reaches 5000 m/s very rapidly (within 30–40 h).

In Fig. 1 are also presented the variations of the percentage of bound water for the different specimens. For each temperature, the variations of $V_L$ and the percentage of bound water occur at the same time. It means that, as it has been shown for velocity and percentage of bound water data between 0 and 24 h, $V_L$ is a parameter which enables us to follow in situ the massive formation of hydrates. For each temperature, specimens have been analysed at different times by DTA (Fig. 2) and XRD (Fig. 3). Table 1 presents for increasing setting times and temperatures the nature of hydrates detected by

DTA or XRD when crystallised. For the hydrates that are crystalline, $\Delta 2\theta$, the width at half height, has been determined (Table 2). The porous volume fraction corresponding to different temperatures and increasing time are given in Table 3. Fig. 4a–c presents the corresponding pore size distributions.

Given all these experimental results, we can consider three different cases which are linked with the different conservation conditions.

### 3.1. Ageing at 5 °C

At 24 h and according to DTA data, the hydrates which are present are $CAH_{10}$ and $AH_3$ (Fig. 2a). $CAH_{10}$ is crystalline and Table 2 shows that $\Delta 2\theta$ ($CAH_{10}$) does not change very significantly during 3500 h. $AH_3$ is not detected by XRD until 3500 h (Fig. 3a), either because the $AH_3$ crystals are too small or $AH_3$ is amorphous. Concerning $C_2AH_8$, it is detected at 3500 h by DTA but not by XRD. It means that it is formed later during the hydration process and remains either amorphous or forms very small crystallites. In these samples, $P$ increases by a few percents with time (Table 3). At 24 h, the pore size distribution is centred around 0.05 μm. It shifts towards higher values with time; at 700 and 3500 h, the average pore size is about 0.15 and 0.2 μm, respectively (Fig. 4a).

### 3.2. Ageing at 20 °C

At 20 °C, $CAH_{10}$, $C_2AH_8$ and $AH_3$ are always present (Table 1, Figs. 2b and 3b). $CAH_{10}$ and $C_2AH_8$ are crystalline. $AH_3$ is detected in the crystalline form at 3500 h. It means that for this particular hydrate, though it is formed very early, its transformation from an amorphous to a crystalline state is slow. In the particular case of $CAH_{10}$, $\Delta 2\theta$ at 3500 h and 20 °C is smaller than $\Delta 2\theta$ at 3500 h and 5 °C. If we assume simply that $\Delta 2\theta$ is inversely proportional to the crystal size, this change in $\Delta 2\theta$ with temperature could be explained by a thermal activation of the growths or coalescence of hydrate.

The variations of $P$ for samples aged at 20 °C are quite different from what has been recorded for samples aged at 5 °C. First of all, $P$ does not change very much between 24 and 55 h (Table 3) and the pore size is located between 0.08 and 0.1 μm (Fig. 4b). Secondly, $P$ decreases at 100 and 250 h but the average pore size remains the same. Lastly, at 700 h, we obtain $P = 0.054$ and the pore size is lower than 0.01 μm. There is a noticeable decrease of these two parameters compared to earlier and it looks as if the porosity was filled by hydrates. At this point in time of the hydration process $V_L$ values become quite high, ≈5000 m/s.

### 3.3. Ageing at 40 and 60 °C

Hydration at these temperatures leads very quickly to the formation of the stable hydrate $C_3AH_6$. A new endothermic peak is observed due to another phase such as carboaluminate $\left(C_4A\overline{C}H_{13}\right)$. The presence of carbon has been evidenced by EDS analysis (Fig. 5). This carboaluminate can be formed by reaction between $C_3AH_6$, $CO_2$ and water.[10,11]

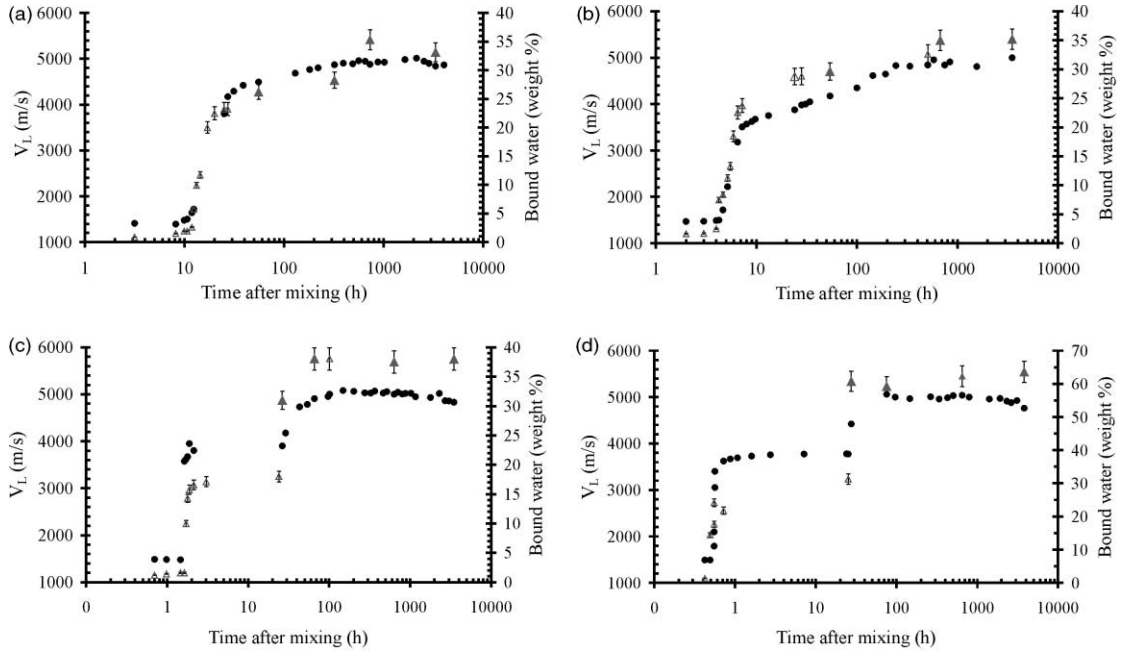


Fig. 1. Variations of $V_L$ and bound water as a function of time for the specimens prepared with $W/C = 0.33$ at different temperatures: (a) 5 °C (specimen 05.033), (b) 20 °C (specimen 20.033), (c) 40 °C (specimen 40.033), (d) 60 °C (specimen 60.033). Symbols: (■) $V_L$; (Δ) bound water; (▲) time at which specimens have been analysed ex situ by TGA and XRD.

For these two temperatures, $\Delta 2\theta$ for $AH_3$ and $C_3AH_6$ remains fairly constant and equal to 0.45–0.50° for $AH_3$, and 0.15–0.18° for $C_3AH_6$. Again, if we assume that $\Delta 2\theta$ in a first approximation is inversely proportional to the crystal size, $AH_3$ crystals would be smaller than $C_3AH_6$ crystals, which as already been reported in the literature.[12] Porosimetric measurements on these samples indicate that the pore size and the pore volume fraction decrease rapidly. Data recorded on the sample at 24 h show that $P$ is equal to 0.215 and the average

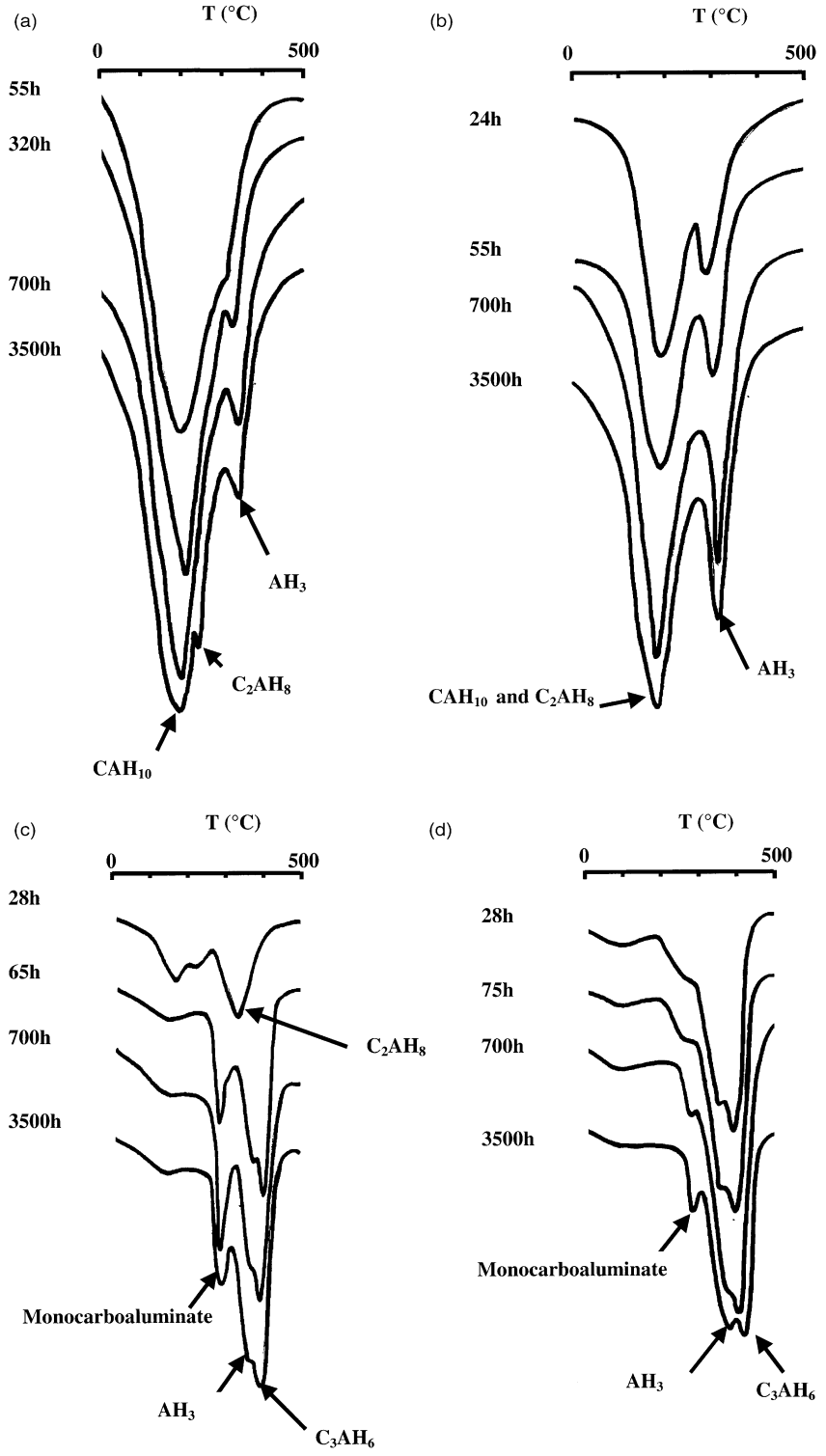


Fig. 2. DTA diagrams for the specimens prepared with $W/C = 0.33$ at different temperatures and for increasing times up to 3500 h: (a) 5 °C (specimen 05.033), (b) 20 °C (specimen 20.033), (c) 40 °C (specimen 40.033), (d) 60 °C (specimen 60.033).

pore size is of the order of 0.8 μm. Beyond this time, $P$ goes down to 0.055 μm and the average pore size is less than 0.01 μm.

### 3.4. Discussion of $V_L$–P data

We have plotted on the same diagram $V_L$ variations as a function of pore volume fraction, $P$ (Fig. 6). The reason for such a plot is that, in the literature describing mechanical characteristics of ceramic based materials, the authors usually plot the variations of mechanical parameters as a function of $P$.[13,14]

In the present case, we notice that for experiments at 40 °C (or 60 °C), there is a good linear relationship between $V_L$ and $P$. Moreover, in the case of the sample aged at 40 °C (or 60 °C), $\Delta 2\theta$ remains fairly constant between 24 and 3500 h. It means there is no significant morphological change during this period. Therefore, $V_L$ seems to depend essentially upon $P$. In order to predict the elastic properties of materials, numerical approaches

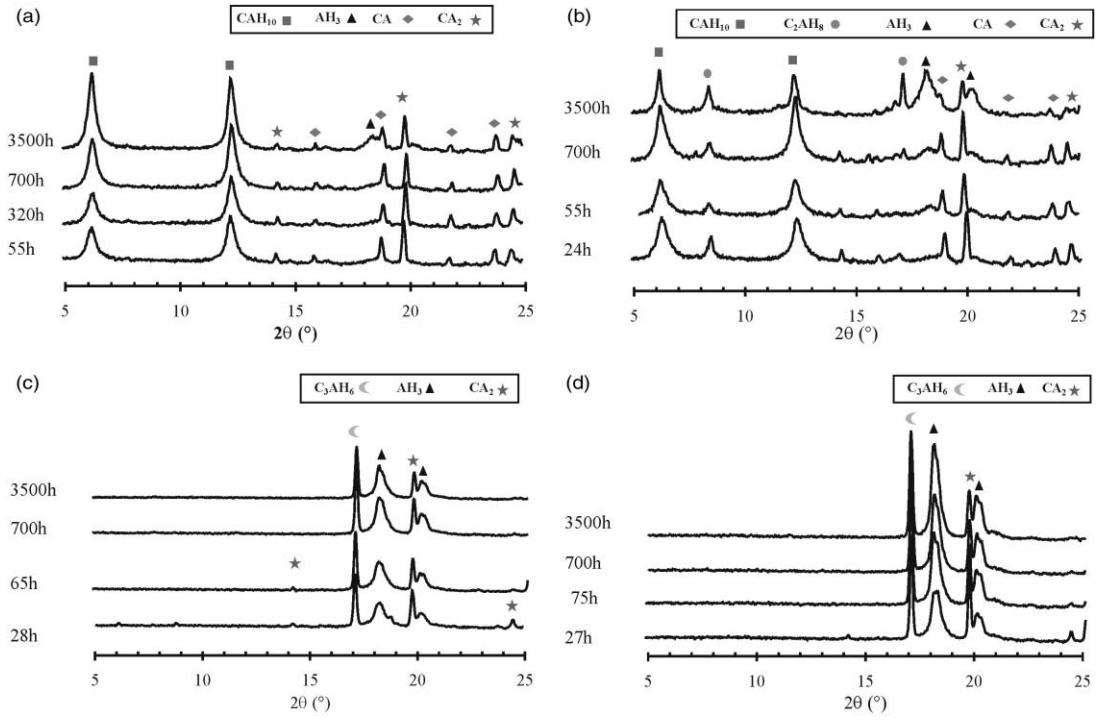


Fig. 3. XRD diagrams for the specimens prepared with $W/C = 0.33$ at different temperatures and for increasing times up to 3500 h: (a) 5 °C (specimen 05.033), (b) 20 °C (specimen 20.033), (c) 40 °C (specimen 40.033), (d) 60 °C (specimen 60.033).

Table 1
Type of hydrates formed at different temperatures from 24 to 3500 h (5 months)

| Specimen | Time after mixing (h) | DTA (amorphous and crystallised phases) | XRD (crystallised phase) |
|---|---|---|---|
| 05.033 | 55 | $CAH_{10}$ and $AH_3$ | $CAH_{10}$ |
| | 320 | $CAH_{10}$ and $AH_3$ | $CAH_{10}$ |
| | 700 | $CAH_{10}$ and $AH_3$ | $CAH_{10}$ |
| | 3500 | $CAH_{10}$, $C_2AH_8$ and $AH_3$ | $CAH_{10}$ and $C_2AH_8$ |
| 20.033 | 24 | $CAH_{10}$, $C_2AH_8$ and $AH_3$ | $CAH_{10}$ and $C_2AH_8$ |
| | 55 | $CAH_{10}$, $C_2AH_8$ and $AH_3$ | $CAH_{10}$ and $C_2AH_8$ |
| | 700 | $CAH_{10}$, $C_2AH_8$ and $AH_3$ | $CAH_{10}$ and $C_2AH_8$ |
| | 3500 | $CAH_{10}$, $C_2AH_8$ and $AH_3$ | $CAH_{10}$ and $C_2AH_8$ and $AH_3$ |
| 40.033 | 28 | $C_2AH_8$, $C_3AH_6$, $AH_3$ | $C_2AH_8$, $C_3AH_6$ and $AH_3$ |
| | 65 | $C_3AH_6$ and $AH_3$ | $C_3AH_6$ and $AH_3$ |
| | 700 | $C_3AH_6$ and $AH_3$ | $C_3AH_6$ and $AH_3$ |
| | 3500 | $C_3AH_6$ and $AH_3$ | $C_3AH_6$ and $AH_3$ |
| 60.033 | 28 | $C_3AH_6$ and $AH_3$ | $C_3AH_6$ and $AH_3$ |
| | 75 | $C_3AH_6$ and $AH_3$ | $C_3AH_6$ and $AH_3$ |
| | 700 | $C_3AH_6$ and $AH_3$ | $C_3AH_6$ and $AH_3$ |
| | 3500 | $C_3AH_6$ and $AH_3$ | $C_3AH_6$ and $AH_3$ |

have been developed on model systems with pores of controlled shapes.[13] The literature also contains data about the variations of elastic properties in polycrystalline oxides such as $Al_2O_3$,[15–18] MgO,[19] ZnO[20] or Portland cements.[21] These data show a linear dependence between Young's modulus, $E$, and $P$, provided $P<0.15$–0.20. Soroka et al.[22] have proposed the following linear relationship:

$$\mathrm{Log}E = \mathrm{Log}E_0 + n\mathrm{Log}(1-P) \quad (2)$$

Assuming in a first approximation that $V_L$ is proportional to $E^{\frac{1}{2}}$ we obtain:

$$\mathrm{Log}V_L = \mathrm{Log}V_0 + \frac{n}{2}\mathrm{Log}(1-P) \quad (3)$$

$V_0$ (resp. $E_0$) corresponds to the longitudinal velocity (resp. Young's modulus) at zero porosity. For all the measurements carried out at 40 °C, Eq. (3) gives $n=2.86$ and $V_0=5340$ m/s. This $n$ value is close to what has been found by Soroka on gypsum which is another hydraulic binder and where $0.1\ 1<P<0.27$.

Table 2
Half-height width of diffraction rays at $2\theta=12.362°$, 8.256°, 17.271° and 18.282° for $CAH_{10}$, $C_2AH_8$, $C_3AH_6$ and $AH_3$ hydrates, respectively, as a function of time and for the specimens prepared with $W/C=0.33$ at 5 °C (specimen 05.033), at 20 °C (specimen 20.033), at 40 °C (specimen 40.033) and at 60 °C (specimen 60.033)

| | Specimen | | | | | | |
|---|---|---|---|---|---|---|---|
| | 05.033 | 20.033 | | 40.033 | | 60.033 | |
| Time (h) | $\Delta 2\theta$ ($CAH_{10}$) | $\Delta 2\theta$ ($CAH_{10}$) | $\Delta 2\theta$ ($C_2AH_8$) | $\Delta 2\theta$ ($C_3AH_6$) | $\Delta 2\theta$ ($AH_3$) | $\Delta 2\theta$ ($C_3AH_6$) | $\Delta 2\theta$ ($AH_3$) |
| 24 | – | 0.37 | 0.26 | 0.18 | 0.46 | – | – |
| 28 | – | – | – | – | – | 0.15 | 0.48 |
| 45 | – | – | – | 0.16 | 0.55 | – | – |
| 55 | 0.35 | 0.31 | 0.29 | – | – | – | – |
| 65 | – | – | – | 0.16 | 0.53 | – | – |
| 75 | – | – | – | – | – | 0.15 | 0.49 |
| 100 | – | – | – | 0.18 | 0.52 | – | – |
| 320 | 0.35 | – | – | – | – | – | – |
| 600 | – | – | – | 0.18 | 0.46 | – | – |
| 700 | 0.33 | 0.32 | 0.28 | 0.16 | 0.48 | 0.15 | 0.48 |
| 3000 | – | – | – | 0.15 | 0.52 | – | – |
| 3500 | 0.33 | 0.24 | 0.22 | 0.16 | 0.39 | 0.15 | 0.48 |

Table 3
Porous volume fraction, $P$, for the different specimens at increasing times

| | Specimen | | |
|---|---|---|---|
| | 05.033 | 20.033 | 40.033 |
| Time (h) | $P$ | $P$ | $P$ |
| 24 | 0.154 | 0.266 | 0.215 |
| 29 | – | – | 0.121 |
| 45 | – | – | 0.075 |
| 55 | – | 0.246 | – |
| 65 | – | – | 0.056 |
| 100 | – | 0.147 | – |
| 250 | – | 0.145 | – |
| 700 | 0.155 | 0.054 | 0.055 |
| 3500 | 0.182 | – | – |

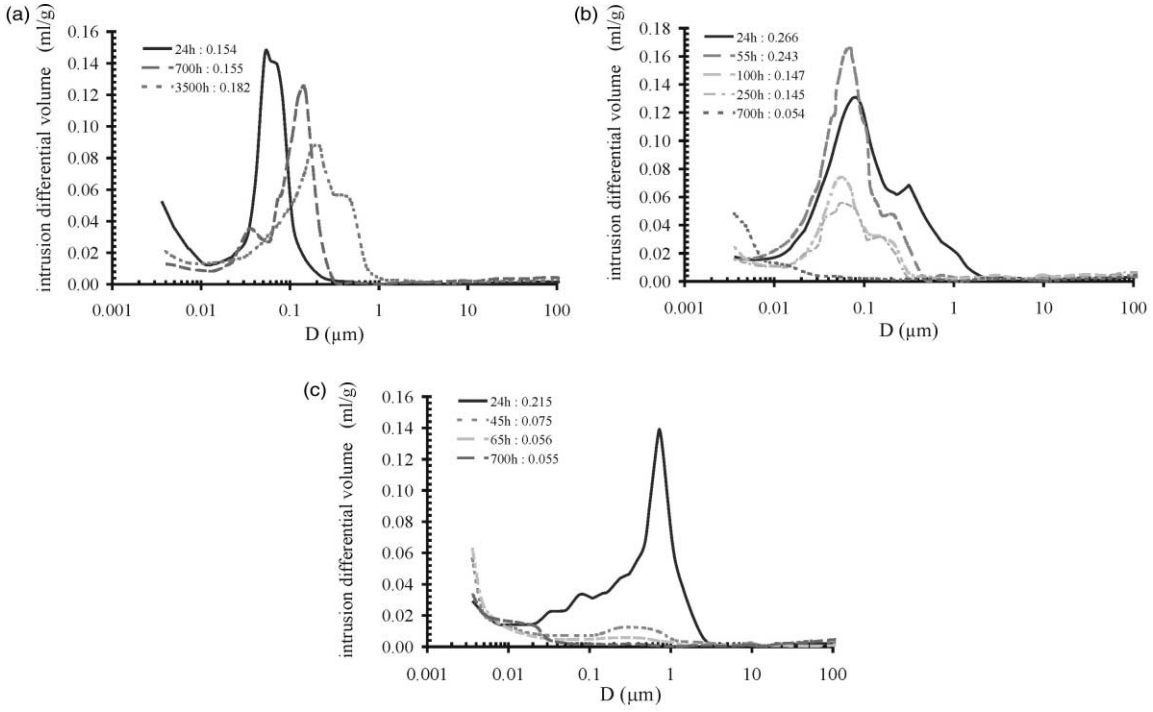


Fig. 4. Pore distribution and pore volume fraction P for the specimens prepared with $W/C=0.33$ at different temperatures and for increasing times: (a) 5 °C (specimen 05.033), (b) 20 °C (specimen 20.033), (c) 40 °C (specimen 40.033).

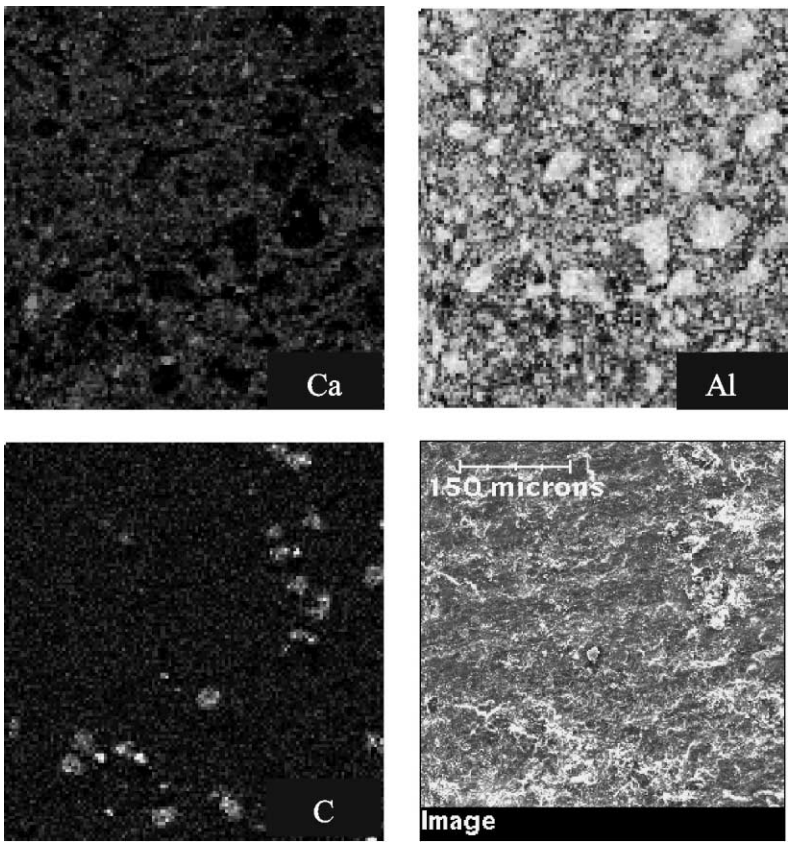


Fig. 5. Result of EDS analysis for a specimen prepared with $W/C=0.33$ at 40 °C (specimen 40.033) and stored in water at 40 °C during 500 h.

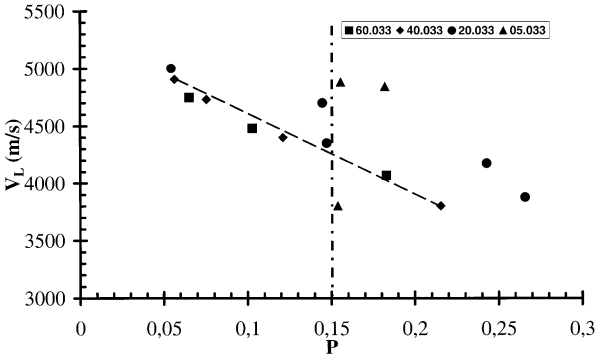


Fig. 6. $V_L$ as a function of the porous volume fraction, $P$, for the specimens prepared with $W/C=0.33$ at 5 °C (specimen 05.033), 20 °C (specimen 20.033), 40 °C (specimen 40.033) and at 60 °C (specimen 60.033).

At 5 °C, there is no obvious relation between $V_L$ and $P$. $V_L$ changes significantly with setting time while $\Delta 2\theta$ stays constant and $P$ only evolves by 18%. The chemical nature of interfaces existing between the different phases probably has an influence on the propagation of the longitudinal waves. Table 4 shows for two times three microstructural parameters: the porous volume fraction ($P$), the bulk density ($\rho_{bulk}$) which considers the solid and the closed porosity, and the apparent density ($\rho_{app}$) which includes the open porosity. Between 24 and 700 h, $V_L$ goes from 3800 up to 4530 m/s while hydration is still progressing. In the same time interval, $P$, associated to the open porosity, stays constant and the two densities increase by 5%. Since the density of hydrates is lower than the density of anhydrous phases, the increase of $\rho_{bulk}$ can be due to a decrease of the closed pores volume. Therefore, during ageing, there would be a better chemical contact between the different phases and this could be responsible for a better propagation of the waves resulting in higher values of $V_L$ at 700 h compared to $V_L$ at 24 h.

Table 4
Values of the porous volume fraction ($P$), the bulk density ($\rho_{bulk}$), and the apparent density ($\rho_{app}$) for the specimens prepared with $W/C=0.33$ at 5 °C (specimen 05.033) at selected times

| Time (h) | $V_L$ (m/s) | $P$ | $\rho_{bulk}$ (g/cm$^3$) | $\rho_{app}$ (g/cm$^3$) |
|---|---|---|---|---|
| 24 | 3800 | 0.154 | 2.34 | 1.98 |
| 700 | 4530 | 0.155 | 2.47 | 2.08 |

At 20 °C, the $P$–$V_L$ can be compared to what has been observed at either 40 °C (and 60 °C) or 5 °C (Fig. 6). When $P<0.15$, we are again in the case where $V_L$ increases when $P$ decreases. The difference with the behaviour at 40–60 °C is that $\Delta 2\theta$ diminishes between 700 and 3500 h. If this is correlated with a growth of hydrated phases, these crystals could fill up the pores.

When $P > 0.15$, it is interesting to compare the data obtained at 20 °C with these collected at different temperatures. For instance, in the case of an ageing at 20 °C and for the specimen where $P = 0.26$, we obtain $V_L = 3800$ m/s. When ageing is done at 40 and 5 °C, similar $V_L$ values are obtained for $P = 0.21$ and 0.15, respectively. It shows that $V_L$ is sensitive not only to porosity but to other factors amongst which we can quote chemical interfaces between phases, nature of hydrates, morphology (shape and size of crystals), microstructure (porosity, tortuosity). It is very difficult to separate the contribution of each parameter. One solution could be to work on "model materials" where the effect of a single parameter would be isolated and the associated ultrasonic behavior studied.

## 4. Conclusion

This study on the ageing behaviour (between 24 and 3500 h) of an aluminous cement ($W/C = 0.33$) at different temperatures (5, 20, 40 and 60 °C) leads to the following points:

(i) the chemical nature of hydrates depends on temperature and time. In particular, at 5 °C, stable $C_3AH_6$ does not form during this interval while at 40 or 60 °C, $C_3AH_6$ is detected very early;
(ii) crystal growth is thermally activated;
(iii) with respect to $V_L$–$P$ variations, we can distinguish two regions. For $P > 0.15$, and $V_L < 4300$ m/s, $V_L$ is sensitive to parameters such as porosity, chemical interfaces between phases, nature of hydrates, morphology (shape and size of crystals), microstructure (porosity and tortuosity). When for $P < 0.15$, and $V_L > 4300$ m/s, $V_L$ is essentially dependent on $P$. In this last case, the elastic properties of the aluminous cement can be described by models developed for single oxides with low porosity.

One possible application of this technique would be to use it in order to assess the durability of aluminous cement based materials in different environmental conditions.

## References

1. Nonnet, E., Lequeux, N. and Boch, P., Elastic properties of high alumina cement castables from room temperature to 1600 °C. *J. Eur. Ceram. Soc.*, 1999, **19**, 1575–1583.
2. Neville, A. M., *Properties of Concrete*. 4th edn. Longman, London, 1995.
3. Chotard, T. J., Gimet-Bréart, N., Smith, A., Fargeot, D., Bonnet, J. P. and Gault, C., Characterisation of calcium aluminate cement hydration at young age by ultrasonic testing. In *Calcium Aluminate Cements*, ed. R. J. Mangabhai and F. P. Glasser. IOM Communications, London, 2001, pp. 155–167.
4. Chotard, T. J., Gimet-Bréart, N., Smith, A., Fargeot, D., Bonnet, J. P. and Gault, C., Application of ultrasonic testing to describe the hydration of calcium aluminate cement at the early age. *Cem. Concr. Res.*, 2001, **31**, 405–412.
5. Smith, A., Chotard, T. J., Gimet-Bréart, N. and Fargeot, D., Correlation between hydration mechanism an ultrasonic measurements in an aluminous cement: effect of setting time and temperature on the early hydration. *J. Eur. Ceram. Soc.,* 2002, **22**(12), 1947–1958.
6. Bachiorrini, A. and Guilhot, B., Premières echéances de l'hydratation de l'aluminate monocalcique: influence du protocole de stoppage. *Cem. Concr. Res.*, 1982, **12**, 557–567.
7. Beaudoin, J. J., Porosity measurement of some hydrated cementitous systems by high pressure mercury intrusion-microstructural limitations. *Cem. Concr. Res.*, 1979, **9**(6), 771–781.
8. Parcevaux, P., Pore size distribution of Portland cement slurries at very early stages of hydration: influence of curing temperature and pressure. *Cem. Concr. Res.*, 1984, **14**(3), 419–430.
9. Diamond, S., Mercury porosimetry, an inappropriate method for the measurement of pore size distributions in cement-based materials. *Cem. Concr. Res.*, 2000, **30**(10), 1517–1525.
10. Midgley, H. G. and Midgley, A., The conversion of high alumina cement. *Mag. of Concr. Res.*, 1975, **27**(91), 59–77.
11. Goni, S., Andrade, C., Sagrera, J. L., Hernandez, S. and Alonso, C., A new insight on alkaline hydrolysis of calcium aluminate cement concrete: part I. Fundamentals. *J. Mater. Res.*, 1996, **11**(7), 1748–1754.
12. Cottin, B., Étude au Microscope Électronique de Pâtes de Ciment Alumineux Hydratées en $C_2AH_8$ et $CAH_{10}$. *Cem. Concr. Res.*, 1971, **1**, 177–186.
13. Rice, R. W., The porosity dependence of physical properties of materials: a summary review. *Key Eng. Mater.*, 1996, **115**, 1–20.
14. Ramakrishnan, N. and Arunnachalam, V. S., Effective elastic moduli of porous ceramic materials. *J. Am. Ceram. Soc.*, 1993, **76**, 2745–2752.
15. Munro, R. G., Effective medium theory of the porosity dependence of bulk moduli. *J. Am. Ceram. Soc.*, 2001, **84**(5), 1190–1192.
16. Roberts, A. P. and Garboczi, E. J., Elastic properties of model porous ceramics. *J Am. Ceram. Soc.*, 2000, **83**(12), 3041–3048.
17. Spriggs, R. M., Brissette, L. A. and Vasilos, T., Effect of porosity on elastic and shear moduli of polycrystalline magnesium oxide. *J. Am. Ceram. Soc.*, 1962, **45**(8), 400.
18. Spriggs, R. M., Effect of open and closed pores on elastic moduli of polycristalline alumina. *J. Am. Ceram. Soc.*, 1962, **45**(9), 454.
19. Spriggs, R. M. and Brissette, L. A., Expressions for shear modulus and Poisson's ratio of porous refractory oxides. *J. Am. Ceram. Soc.*, 1962, **45**(4), 198.
20. Martin, L. P. and Rosen, M., Correlation between surface area reduction and ultrasonic velocity in sintered zinc oxide powders. *J. Am. Ceram. Soc.*, 1997, **80**(4), 839–846.
21. Cook, R. A. and Hover, K. C., Mercury porosimetry of hardened cement pastes. *Cem. Concr. Res.*, 1999, **29**, 933–943.
22. Soroka, I. and Sereda, P. J., Interrelation of hardness, modulus of elasticity, and porosity in various gypsum systems. *J. Am. Ceram. Soc.*, 1968, **51**, 337–340.